

Addressable micropost array for the dielectrophoretic manipulation of particles in fluid

T. P. Hunt, H. Lee, and R. M. Westervelt^{a)}

Department of Physics and Division of Engineering and Applied Sciences, Harvard University, Cambridge, Massachusetts 02138

(Received 6 April 2004; accepted 25 October 2004)

A microfluidic device has been developed to trap and position neutral particles using dielectrophoresis. An array of microscale post shaped electrodes provides an inhomogeneous electric field. The voltage on each electrode can be independently controlled by a computer to trap and move particles in fluid above the micropost electrodes. Yeast cells and polystyrene spheres were trapped and moved, demonstrating both positive and negative dielectrophoresis. © 2004 American Institute of Physics. [DOI: 10.1063/1.1840109]

Dielectrophoresis (DEP) is a well-known technique for manipulating neutral particles in fluid.^{1–5} Much investigation has gone into the performance of traps with fixed field geometries^{6–8} and their use for electrical characterization⁹ and separation^{10–13} of cells and particles. Electric-field gradients for DEP traps are generated by microfabricated electrodes that produce local electric fields¹⁴ or by microfabricated insulators that alter the flow of ions in solution.¹⁵ An array of traps with independent addressable electrodes provides a more flexible and powerful manipulation system than traps with fixed electric field geometries.¹⁶ An addressable array of closely spaced electrodes is capable of transporting cells or particles across the array.¹⁷ Combining an array of addressable electric traps with microfluidic channels allows the creation of a programmable microfluidic system that can independently control the motion of many cells at once.

In this letter, we describe a micropost matrix, which is a two-dimensional array of post shaped electrodes combined with a microfluidic channel. The micropost matrix is capable of versatile manipulation of particles and cells using DEP. Each electrode is independently addressable by an analog voltage source, which allows fine control of the trapping field inside the microfluidic channel. With the electric field produced by the micropost matrix, cells and polystyrene beads were trapped and transported inside a microfluidic channel. The union of microfluidics and a matrix of DEP traps creates a device capable of manipulation, separation, and assembly of individual cells.

The DEP force on a polarizable particle arises from the interaction between an inhomogeneous electric field and the dipole induced on the particle. The DEP force on a spherical particle is $F_{\text{DEP}} = 2\pi\epsilon_f r^3 \text{Re}[CM(\omega)] \nabla E_{\text{rms}}^2$, where r is the radius of the particle, E_{rms} is the root-mean-squared (rms) electric field, ϵ_f is the fluid permittivity, $CM(\omega)$ is the Clausius–Mossotti factor, and ω is the frequency of the electric field. $CM(\omega)$ is dependent on the relative permittivity and conductivity of the particle and the fluid,² and it can vary between -0.5 and 1 . When $CM(\omega) < 0$, the fluid is more polarizable than the particle, and the particle is pulled toward the local minimum of the electric field. This is called negative DEP (nDEP). Positive DEP (pDEP) occurs when the particle is more polarizable than the fluid, $CM(\omega) > 0$, and

the particle is pulled to the maximum of the electric field. DEP takes advantage of ac fields to minimize both the voltage across biological cell membranes and the electro-osmotic flow of the charged double layer.³ By controlling the frequency, fluid conductivity, and electric-field distribution, it is possible to trap a given particle with either nDEP or pDEP.

The micropost matrix shown in Fig. 1 uses post shaped electrodes to concentrate the electric field lines under the cells in the fluid. Figure 1(a) shows a micrograph of the micropost matrix, and Fig. 1(b) shows the layout of the microposts in three dimensions. The posts help to isolate the cells from electric fields produced by the leads. A schematic cross-sectional view of the device is provided in Fig. 1(c). The post shaped electrodes function as an array of monopoles that can be charged with different analog voltages—the field lines go from the posts to a conducting cover plate.

The micropost matrix was constructed on a glass substrate. Electrical leads were defined by liftoff of a metal layer (7.5 nm Ti, 50 nm Au) following photolithographic patterning. A thick (10 μm) layer of biocompatible resist, SU-8 (Microchem), was used to pattern a mold for electrodeposition of the gold microposts. A dilute HF dip was used prior to

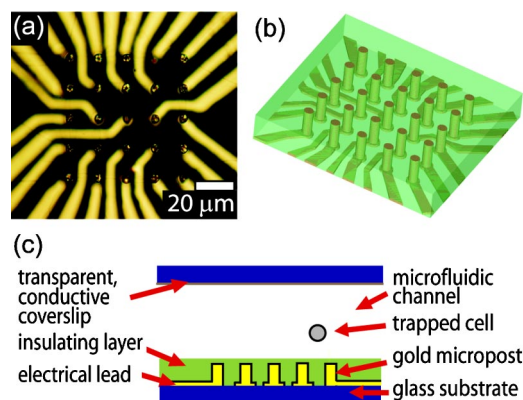


FIG. 1. (Color online) Micrograph and schematic diagram of the micropost matrix. (a) Micrograph of the micropost matrix. The tops of the posts are in the focal plane, the electrical leads are below the focal plane, and the insulating SU-8 is transparent. (b) Three-dimensional drawing showing the design of the micropost matrix. (c) Cross-sectional schematic of the device. The micropost matrix is composed of gold leads with 10 μm high post shaped electrodes on top of them. The array of electrodes is capped with a 2 μm thick insulating layer. The array of electrodes forms the bottom of a 45 μm high fluidic chamber that is sealed with a conductive coverslip.

^{a)}Electronic mail: westervelt@deas.harvard.edu

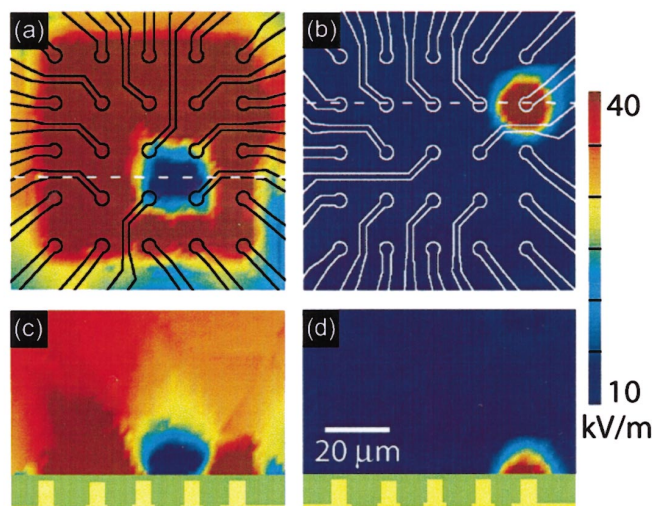


FIG. 2. (Color) Electric-field simulations of trapping fields created by the micropost matrix. (a) Electric-field pattern in a plane located $8\ \mu\text{m}$ above the top of the posts showing a minimum for nDEP trapping. (b) Electric-field pattern in a plane located $4\ \mu\text{m}$ above the top of the posts showing a maximum for pDEP trapping. (c) Cross section of the field pattern along the dotted line in (a). (d) Cross section of the field along the dotted line in (b). The actual geometry of the device is outlined in the figure, including the location of the leads and a cross section of the posts.

SU-8 spin coating to improve the adhesion of the SU-8 resist to the glass substrate. The microposts were electrodeposited in gold plating solution, stirred at $70\ ^\circ\text{C}$, with a deposition rate $\sim 3\ \mu\text{m}/\text{h}$. An insulating layer ($2\ \mu\text{m}$ thick) and a fluidic chamber ($45\ \mu\text{m}$ high), both SU-8, were patterned on top of the microposts. Inlet and outlet holes for fluidics were drilled through the substrate with a diamond bit, and the device was glued to a ceramic carrier with matching holes. A glass coverslip was sputter coated with indium tin oxide to produce a conducting layer. The coating had an optical transmittance $>90\%$ and resistance $<1\ \text{k}\Omega$ across the length of the coverslip. The coverslip was sealed on top of the fluidic channel with low viscosity cyanoacrylate (Loctite 408).

Electrical connections were made through aluminum wire bonds to the ceramic carrier, which was inserted in a socket on a circuit board connected to the voltage sources. The socket also provided the fluidic connection through an O-ring seal between the chip carrier and a syringe pump. A computer equipped with analog voltage output channels produced a dc signal for each electrode. The dc signals were individually multiplied with the output of a single function generator to provide an ac voltage to each post with amplitude $V_{\text{post}}=0$ to $10\ \text{V}$ at frequencies up to $\omega=10\ \text{MHz}$. The conductive coverslip was grounded in all of the experiments reported here.

Figure 2 shows simulations of the electric-field patterns produced by the micropost matrix for both pDEP and nDEP trapping. Simulations were performed using a finite element package (Maxwell 3D, Ansoft) on the actual device geometry shown in Fig. 1: Electrical leads, microposts $5\ \mu\text{m}$ in diameter, $10\ \mu\text{m}$ in height and spaced $15\ \mu\text{m}$ center to center, an insulating layer $2\ \mu\text{m}$ thick, a channel $45\ \mu\text{m}$ high filled with water, and a conductive coverslip. The top and side view of a typical nDEP trap simulation are pictured in Figs. 2(a) and 2(c). In the nDEP trap, the minimum of the electric field is formed $8\ \mu\text{m}$ above the top of the posts in Fig. 2(c). In this simulation, the posts on the edge of the

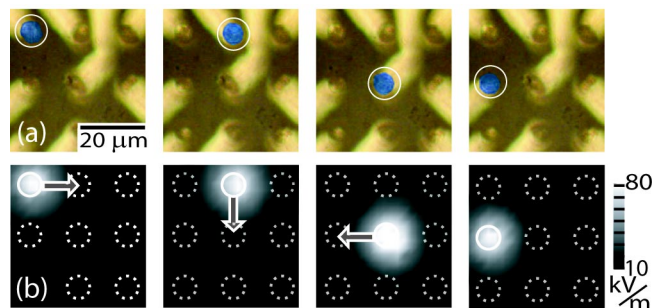


FIG. 3. (Color online) Trapping and manipulation of a single yeast cell with pDEP. (a) A yeast cell (circled, contrast enhanced) is translated clockwise in a square pattern above the micropost matrix. The post shaped electrodes, $5\ \mu\text{m}$ in diameter, are spaced $15\ \mu\text{m}$ center to center. (b) Electric-field simulations of the trapping field acting on the yeast cell in each location. The yeast is pulled into the maximum of the electric field. The simulation plane is $2\ \mu\text{m}$ above the bottom of the chamber, close to the center of the trapped yeast cell. Arrows indicate direction of trap motion. The locations of energized micropost electrodes are circled in white; grounded electrodes are circled in dotted white.

matrix were energized with $V_{\text{post}}=10\ \text{V}$ while a local field minimum was created between four grounded inner posts and the grounded conductive coverslip. Figures 2(b) and 2(d) show the top and side views of a pDEP trap simulation. One post is energized with $V_{\text{post}}=10\ \text{V}$ while the remainder are grounded. The maximum of the electric field is directly above the energized post. These simulations show that the field from the leads in the microfluidic channel is small compared with the field created by the microposts, because the leads are located $10\ \mu\text{m}$ below the top of the microposts. If multiple electrodes are energized at the same time, the micropost matrix can produce multiple electric field peaks. In addition, through the use of a thicker insulating layer and two posts at different analog voltages, it would be possible to continuously translate the position of the field maximum between two posts.

Figure 3 shows pDEP trapping and manipulation of a single yeast cell. Micrographs of the trapped cell are shown in Fig. 3(a) while corresponding simulations of the trapping field are shown in Fig. 3(b). Bakers yeast (*Saccharomyces cerevisiae*) was mixed in a solution of distilled water and $100\ \text{mM}$ mannitol. Yeast cells were injected into the micro fluidic channel by a syringe pump and a single cell was trapped in the maximum of the electric field as shown in Fig. 3(a). The center of the trap was moved from one post to another by selectively energizing one post at a time with $V_{\text{post}}=10\ \text{V}$ and $\omega=10\ \text{MHz}$. A simulation of the trapping field corresponding to the cell location in each frame of Fig. 3(a) is shown in Fig. 3(b). The post diameter was designed to be similar to the cell size ($\sim 5\ \mu\text{m}$). The trapped yeast cell followed the electric field maximum with a velocity $\sim 10\ \mu\text{m}/\text{s}$ as the field maximum moved from one post to another. It was also possible to trap and move multiple yeast cells in multiple traps by simultaneously energizing more than one micropost.

Figure 4 shows nDEP trapping of polystyrene beads with the same device used for pDEP. Polystyrene beads ($10\ \mu\text{m}$ diameter, Duke Scientific) were washed in deionized water and injected into the device. Energizing the posts on the edge of the matrix with $V_{\text{post}}=10\ \text{V}$ and $\omega=10\ \text{MHz}$ while the posts in the center of the matrix were grounded, created a local field minimum in the fluidic chamber $\sim 8\ \mu\text{m}$ above

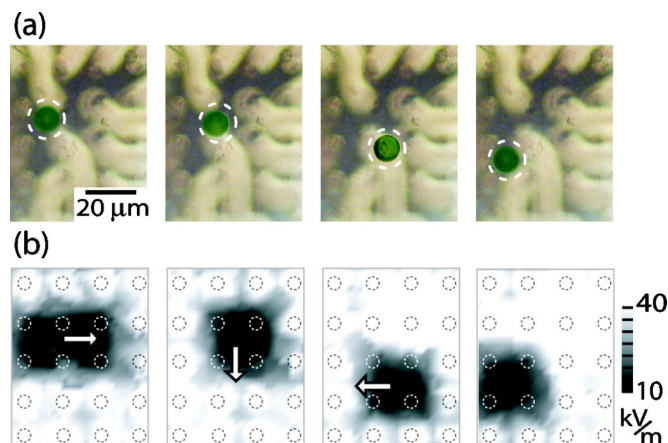


FIG. 4. (Color online) Trapping and manipulation of a single $10\ \mu\text{m}$ diameter polystyrene bead with nDEP. (a) The trapped bead (circled by dotted line, contrast enhanced) follows the minimum of the electric field created by the micropost matrix. (b) Simulation of the field inside the microfluidic channel in a plane located $8\ \mu\text{m}$ above the top of the microposts. The field minimum is produced between the grounded conductive coverslip and the grounded micropost electrodes (location circled in white) surrounded by energized micropost electrodes (location circled in gray). The trap was moved above the matrix by selectively energizing or grounding the microposts. Arrows indicate the direction of trap motion.

the top of the grounded posts. The bead was trapped in the minimum of the electric field. The trap was moved above the matrix by selectively energizing or grounding the inner posts. In Fig. 4(a), a bead follows the nDEP trap as the field minimum is translated across the middle of the matrix. Figure 4(b) shows corresponding simulations of the field patterns that act on the bead in Fig. 4(a). The polystyrene bead was trapped and transported through the fluid above the micropost matrix without bringing it into contact with the bottom of the chamber, an added advantage of nDEP. Continuous transport across the center of the device is possible by applying analog voltages to the posts in the center of the matrix.

In this letter, we have described a micropost matrix and demonstrated trapping and manipulation of cells and particles in a microfluidic channel. The electric fields from the sequentially energized micropost electrodes moved yeast cells and polystyrene beads using positive and negative dielectrophoresis. A two-dimensional addressable array of microelectrodes for DEP manipulation offers the possibility of programmable real time control over the location of cells and particles in a microfluidic system.

The authors thank W. Moss and T. Malliaris for their help. This work was supported by a gift from Philip Morris and by the Nanoscale Science and Engineering Center at Harvard under NSF Grant No. PHY-0117795.

- ¹H. A. Pohl, *Dielectrophoresis* (Cambridge University Press, Cambridge, UK, 1978).
- ²T. B. Jones, *Electromechanics of Particles* (Cambridge University Press, Cambridge, UK, 1995).
- ³M. P. Hughes, *Nanoelectromechanics in Engineering and Biology* (CRC Press, Boca Raton, 2003).
- ⁴D. Bennett, B. Khusid, C. James, P. Galambos, M. Okandan, D. Jacqmin, and A. Acrivos, *Appl. Phys. Lett.* **83**, 4866 (2003).
- ⁵S. W. Lee and R. Bashir, *Appl. Phys. Lett.* **83**, 3833 (2003).
- ⁶J. Voldman, M. Toner, M. L. Gray, and M. A. Schmidt, *J. Electrostat.* **57**, 69 (2003).
- ⁷J. Suehiro and R. Pethig, *J. Phys. D* **31**, 3298 (1998).
- ⁸N. Markarian, M. Yeksel, B. Khusid, and K. Farmer, *Appl. Phys. Lett.* **82**, 4839 (2003).
- ⁹N. G. Green and H. Morgan, *J. Phys. D* **30**, 2626 (1997).
- ¹⁰X. B. Wang, Y. Huang, J. P. H. Burt, G. H. Markx, and R. Pethig, *J. Phys. D* **26**, 1278 (1993).
- ¹¹R. Krupke, F. Henrich, H. Lohneisen, and M. Kappes, *Science* **301**, 344 (2003).
- ¹²G. H. Markx, M. S. Talary, and R. Pethig, *J. Biotechnol.* **32**, 29 (1994).
- ¹³B. H. Lapizco-Encinas, B. A. Simmons, E. B. Cummings, and Y. Fintschenko, *Anal. Chem.*, **76** 1571 (2004).
- ¹⁴M. Washizu and O. Kurosawa, *IEEE Trans. Ind. Appl.* **26**, 1165 (1990).
- ¹⁵C. Chou, J. O. Tegenfeldt, O. Bakajin, S. S. Chan, E. C. Cox, N. Darnton, T. Duke, and R. H. Austin, *Biophys. J.* **83**, 2170 (2002).
- ¹⁶N. Manaresi, A. Romani, G. Medoro, L. Altomare, A. Leonardi, M. Tartagni, and R. Guerrieri, *IEEE J. Solid-State Circuits* **38**, 2297 (2003).
- ¹⁷Y. Huang and R. Pethig, *Meas. Sci. Technol.* **2**, 1142 (1991).